



# Myelin breakdown favours *Mycobacterium leprae* survival in Schwann cells

Bruno Siqueira Mietto<sup>1,2</sup> | Beatriz Junqueira de Souza<sup>2</sup> | Patricia Sammarco Rosa<sup>3</sup> |  
Maria Cristina Vidal Pessolani<sup>2</sup> | Flavio Alves Lara<sup>2</sup> | Euzenir Nunes Sarno<sup>2</sup>

<sup>1</sup> Institute of Biological Sciences, Federal University of Juiz de Fora, Juiz de Fora, Brazil

<sup>2</sup> Oswaldo Cruz Institute, Oswaldo Cruz Foundation, Rio de Janeiro, Brazil

<sup>3</sup> Lauro de Souza Lima Institute, São Paulo, Brazil

## Correspondence

Bruno Siqueira Mietto, Institute of Biological Sciences, Federal University of Juiz de Fora, Juiz de Fora, Brazil.  
Email: bruno.mietto@ufjf.edu.br

## Funding information

FAPERJ; Fiocruz; CAPES; CNPq

## Abstract

Leprosy neuropathy is a chronic degenerative infectious disorder of the peripheral nerve caused by the intracellular obligate pathogen *Mycobacterium leprae* (*M. leprae*). Among all nonneuronal cells that constitute the nerve, Schwann cells are remarkable in supporting *M. leprae* persistence intracellularly. Notably, the success of leprosy infection has been attributed to its ability in inducing the demyelination phenotype after contacting myelinated fibres. However, the exact role *M. leprae* plays during the ongoing process of myelin breakdown is entirely unknown. Here, we provided evidence showing an unexpected predilection of leprosy pathogen for degenerating myelin ovoids inside Schwann cells. In addition, *M. leprae* infection accelerated the rate of myelin breakdown and clearance leading to increased formation of lipid droplets, by modulating a set of regulatory genes involved in myelin maintenance, autophagy, and lipid storage. Remarkably, the blockage of myelin breakdown significantly reduced *M. leprae* content, demonstrating a new unpredictable role of myelin dismantling favouring *M. leprae* physiology. Collectively, our study provides novel evidence that may explain the demyelination phenotype as an evolutionarily conserved mechanism used by leprosy pathogen to persist longer in the peripheral nerve.

## KEYWORDS

disease processes, diseases, infection, metabolism, microbial–cell interaction, mycobacteria

## 1 | INTRODUCTION

Leprosy neuropathy is a chronic degenerative disorder caused by infection of peripheral nerves by *Mycobacterium leprae* (*M. leprae*), an obligate intracellular pathogen with particular ability to invade and persist in Schwann cells (Scollard, Truman, & Ebenezer, 2015; Serrano-Coll, Salazar-Peláez, Acevedo-Saenz, & Cardona-Castro, 2018). Over the past few years, we and others have reported several changes in infected nonmyelinating Schwann cells that favour *M. leprae* survival intracellularly, such as lipid droplets dynamics (Barisch & Soldati, 2017; Elamin, Stehr, & Singh, 2012; Kaur & Kaur, 2017;

Mattos et al., 2010, 2011; Mattos, Sarno, Pessolani, & Bozza, 2012), central glucose metabolism modulation (Medeiros et al., 2016), and cellular reprogramming (Masaki et al., 2013; Petito et al., 2013). Particularly, the success of *M. leprae* infection also includes its natural ability in inducing demyelination after contacting myelinated fibres (Rambukkana, Zanazzi, Tapinos, & Salzer, 2002; Tapinos, Ohnishi, & Rambukkana, 2006). However, the metabolic implication of myelin breakdown for *M. leprae* physiology was entirely ignored.

Myelin is a lipid-rich membrane produced and constantly maintained by Schwann cells in the peripheral nerve (Chrast, Saher, Nave, & Verheijen, 2011). Importantly, during the process of myelin breakdown, the majority of myelin-derived lipids are drawn from the degrading myelin ovoids, then stored in lipid droplets to be later

Dr. Lara and Dr. Sarno should be considered joint senior author.

reused by Schwann cells for de novo synthesis of myelin membranes (Brosius-Lutz et al., 2017; Goodrum, Earnhardt, Goines, & Bouldin, 1994). Due to a massive gene decay that leads to the loss of almost half of the functional genes (Cole et al., 2001), *M. leprae* acquires a unique capacity to subvert the host cell metabolism for its own needs (Elamin et al., 2012; Kaur & Kaur, 2017; Mattos et al., 2012; Medeiros et al., 2016). Typically, effective *M. leprae* survival has been associated with lipid droplets accumulation, a key pathological characteristic also induced by a wide range of intracellular bacterial pathogens (Barisch & Soldati, 2017).

In the light of these evidence, we hypothesised that *M. leprae* would benefit from inducing demyelination, as a way to have access to lipid droplets derived from the process of myelin breakdown.

## 2 | RESULTS

### 2.1 | *M. leprae* infects Schwann cells and accelerates myelin breakdown

Although nonmyelinating Schwann cells have widely been used in *M. leprae* research (Casalenovo et al., 2019; Masaki et al., 2013; Petito et al., 2013), we took advantage of freshly dissociated myelin degrading Schwann cells (hereafter named as mSCs) from mouse peripheral nerves to understand the consequences of *M. leprae* infection for myelin breakdown and clearance in vitro. We first examined the infection rate in our model and noted that the majority of mSCs were positively infected by *M. leprae* (~98%) at day three after incubation (Figure 1a–c). Interestingly, inside mSCs, *M. leprae* was often located in areas enriched in myelin ovoids (Figure 1d), resulting in a significant myelin–*M. leprae* interaction of about 80% in the host cell (Figure 1e).

We next questioned whether *M. leprae* infection would impact the process of myelin breakdown inside mSCs. To answer this, we measured and compared the myelin area in uninfected and *M. leprae*-infected mSCs over a period of time (0, 1, and 3 days) and plotted the results as the per cent of mSCs containing low ( $0\text{--}350 \mu\text{m}^2$ ), medium ( $350\text{--}700 \mu\text{m}^2$ ), or high ( $>700 \mu\text{m}^2$ ) degenerating myelin content. In the uninfected group at 0 hr (starting time point), we observed a distribution of about 27.4%, 40.7%, and 31.8% of mSCs cells in the low, medium, and high myelin ranges, respectively (data not shown). In addition, after 1 and 3 days in vitro, uninfected mSCs presented a gradual reduction of their myelin content as follows: 36.2%, 40.9%, and 22.3% (1 div) and 43.4%, 39.7%, and 16.8% (3 div), respectively, which reflects the natural progressive process of myelin degeneration inside the cell (Figure 1f,g,i,j). Interestingly, *M. leprae*-infected mSCs, at day 1, showed a significant 2.3-fold reduction in the myelin area at high range that reflected in a 1.6-fold increase in the per cent of cells at the low range (Figure 1i). Moreover, at day 3, we observed a marked sixfold (medium range) and twofold (high range) reduction in myelin area that resulted in a substantial increase up to 79% of mSCs containing reduced myelin ovoids (Figure 1h,j). Concurrent with the enhancement on myelin degradation, we also found a statistical reduction in the mRNA levels for myelin basic protein (MBP), myelin protein zero

(MPZ), and KROX-20 in the *M. leprae*-infected group compared with uninfected mSCs (Figure 1k), which is consistent with the ability of *M. leprae* in inducing, since the very early stages, the reprogramming of mSCs to a nonmyelin-producing phenotype. To further analyse changes in myelin transcripts during leprosy infection in vivo, we measured and observed that nerves from leprosy patients have a statistical downregulation of MBP and MPZ mRNA when compared with nonleprosy patients (Figure 1l). Collectively, these data indicate that *M. leprae* is capable of entering mSCs and be clustered around myelin ovoids. Furthermore, this host-pathogen interaction resulted in the acceleration of myelin breakdown that was accompanied by downregulation in a set of key regulatory genes involved in myelin production in vitro and in vivo.

### 2.2 | *M. leprae* enhances the autophagic myelin destruction leading to increased lipid droplets levels

Inside mSCs, myelin ovoids are progressively degraded by macroautophagy mechanisms named as myelinophagy (Gomez-Sanchez et al., 2015; Jang et al., 2016). We therefore focused to understanding whether advanced myelin clearance observed in *M. leprae*-infected cells would be related to changes in this autophagic myelin destruction pathway. To assess this, we first quantified the number of myelin ovoids positive for the autophagosome marker LC3. Although uninfected mSCs presented about 26% of LC3<sup>+</sup> puncta-myelin ovoids, in *M. leprae*-infected cells, we observed a significant increase of up to 82% (threefold more; Figure 2a–c). Accordingly, the mRNA levels of Beclin-1, Wipi2, ULK1, and ATG7 (transcripts involved in the early stages of autophagosome formation) were significantly increased in *M. leprae*-infected mSCs (Figure 2d) as well as in nerve biopsies from leprosy patients (Figure 2e). Because myelin breakdown results in lipid droplets formation (Brosius-Lutz et al., 2017; Goodrum et al., 1994), and knowing the importance of lipids to the intracellular bacteria (Barisch & Soldati, 2017; Elamin et al., 2012; Kaur & Kaur, 2017), we next measured the number of these myelin-derived neutral lipids by oil red O staining (Figure 2f–h) as well as the myelin ovoids size in uninfected and *M. leprae*-infected mSCs at day 3 (Figure 2i). The results of the experiment revealed that although uninfected mSCs exhibited an average of about 5.6 lipid droplets per cell, that number statistically increased three times more in the *M. leprae*-infected group, reaching an average of about 17 oil red O lipid bodies per mSCs (Figure 2h). We also observed a statistical reduction of about 40% in myelin ovoids size in *M. leprae*-infected mSCs (Figure 2i), which correlates very well with the advanced myelin breakdown and lipid droplets arising induced by leprosy infection. Consistent with this, we observed in *M. leprae*-infected mSCs, a marked 8.7-fold induction in perilipin (a lipid droplet-associated protein) mRNA expression as well as a statistical 40% and 55% downregulation in adipose triglyceride lipase (ATGL) and hormone-sensitive lipase (HSL) transcripts (both related to lipolysis), respectively, if compared with values seen in uninfected cells (Figure 2j). Thus, these results indicate an enhancement on myelinophagy leading to increased lipid

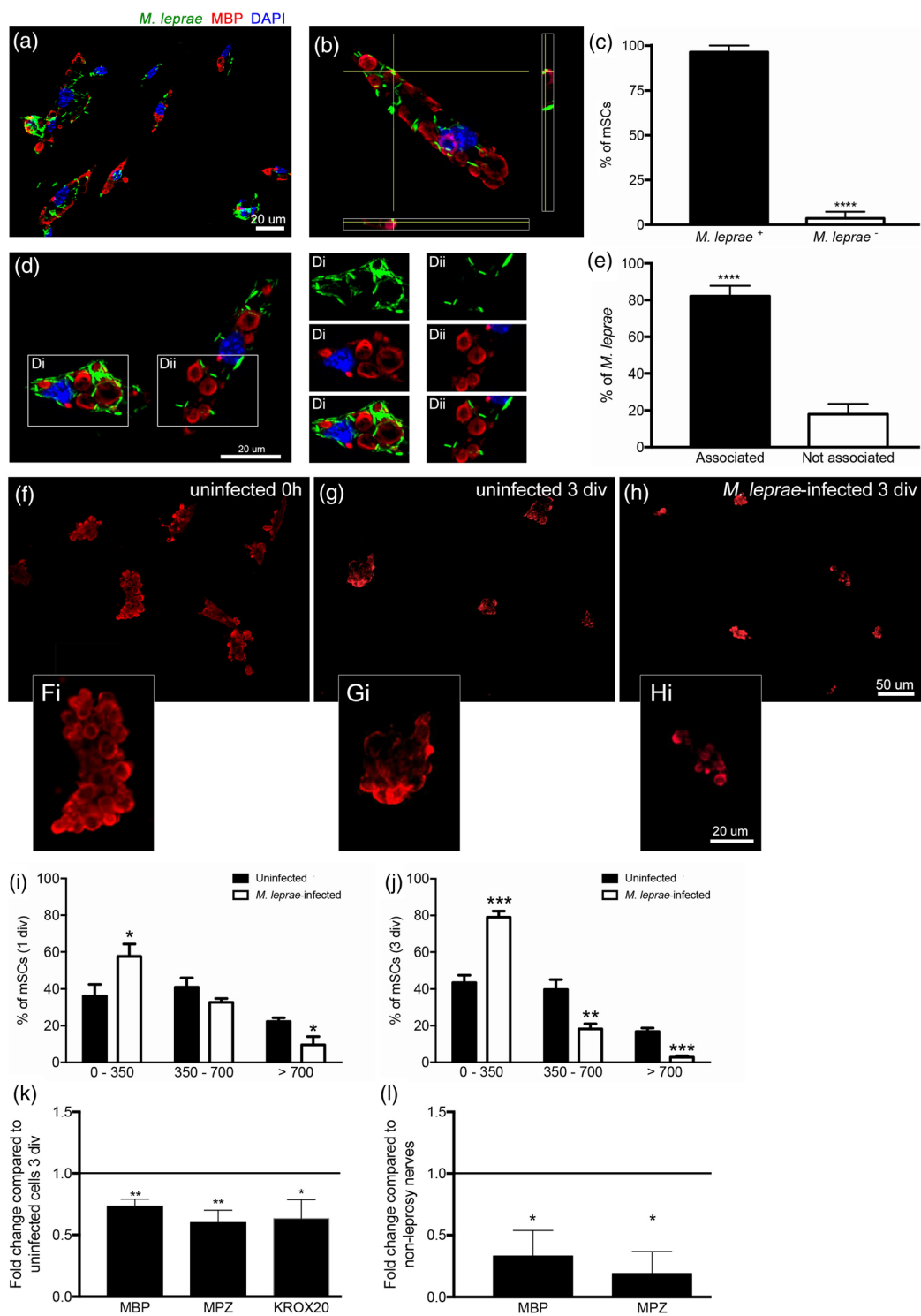


**FIGURE 1** Enhancement of myelin breakdown in response to *M. leprae* entry in Schwann cells. (a, b) Leprosy pathogen successfully invade mSCs and resides in close association with degrading myelin ovoids as indicated at orthogonal sections. (c) The infection rate is expressed as mean  $\pm$  SD from four independent experiments with at least 80 cells counted per experiment. (d) Apotome image of an infected mSCs culture depicting *M. leprae*-myelin interaction at insets. (e) The interaction rate is expressed as mean  $\pm$  SD from four independent experiments with 80 to 200 myelin ovoids counted per each experiment. (f–h) Immunostaining for MBP in mSCs cultures, showing the progressive course of myelin breakdown and clearance in uninfected cells, from day 0 to 3, and the striking reduction induced by leprosy infection. (Fi–Hi) Inset represents example of myelin ovoids content in mSCs over time and at different conditions. (i, j) The graphs show the distribution of mSCs in three distinct myelin area ranges at days 1 and 3, respectively. (k, l) Fold-change analysis showing significantly downregulation of myelin transcripts in vitro (k) and in nerve biopsies from leprosy conditions (l); the horizontal bar represents levels in uninfected conditions; results are expressed as mean  $\pm$  SD from three to four normalised independent biological replicates; \* $p < .5$ , \*\* $p < .01$ , \*\*\* $p < .001$ , \*\*\*\* $p < .0001$ .

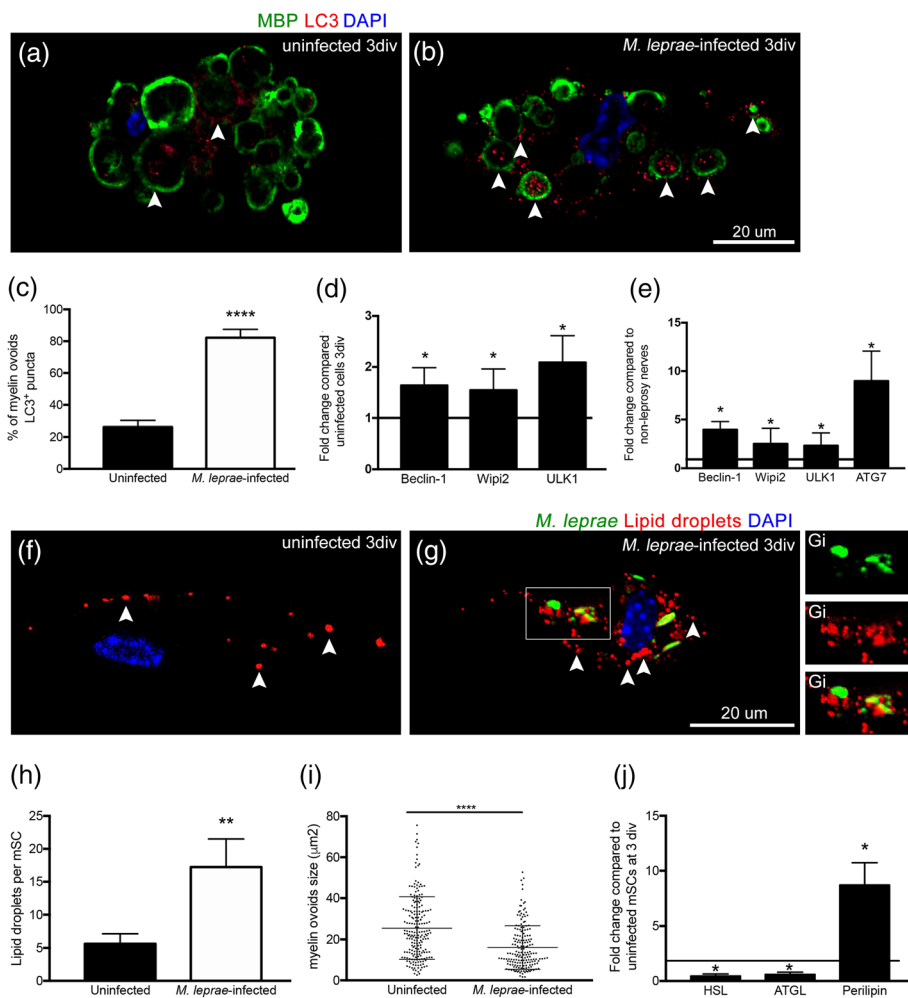


**FIGURE 2** Elevated myelinophagy leads to increased lipid droplets accumulation. (a, b) Representative apotome images showing the accumulation of LC3 puncta in degenerating myelin ovoids (MBP; arrowheads) in uninfected (a) and *M. leprae*-infected (b) mSCs at day 3 in vitro. (c) The graph shows the percentage of LC3-decorated myelin ovoids; results are expressed as mean  $\pm$  SD from three independent experiments with at least 130 myelin ovoids analysed per experiment. (d, e) Fold-change analysis showing significantly upregulated levels for the autophagosome transcripts in vitro (d) and in nerve biopsies from leprosy conditions (e); the horizontal bar represents levels in uninfected conditions; results are expressed as mean  $\pm$  SD from three to four normalised independent biological replicates; (f, g) Oil red O staining showing lipid droplets (arrowheads) in uninfected (f) and *M. leprae*-infected mSCs (g). (Gi) Insets show lipid droplets–*M. leprae* association. (h) Quantification of lipid droplets numbers per mSCs; results are expressed as mean  $\pm$  SD from three independent experiments with at least 40 mSCs analysed per experiment. (i) quantification of myelin ovoids size in uninfected and *M. leprae*-infected mSCs; results are expressed as mean  $\pm$  SD from three independent experiments with at least 100 myelin ovoids counted per each experiment. (j) qRT-PCR showing changes in the mRNA levels for HSL, ATGL, and perilipin in *M. leprae*-infected mSCs compared with uninfected mSCs (horizontal bar) at day 3; results are expressed as mean  $\pm$  SD from three normalised independent biological replicates.  $^*p < .5$ ,  $^{**}p < .01$ ,  $^{***}p < .0001$

droplets formation as a response of *M. leprae* infection in mSCs, which was also followed by upregulation of transcripts involved in autophagosome formation and lipid droplets accumulation.

### 2.3 | Myelin breakdown favours *M. leprae* viability inside Schwann cells

If myelin breakdown benefits leprosy pathogen, preventing myelin from degradation should reduce its viability. We therefore pharmacologically inhibited myelin degeneration by treating mSCs cultures with JNK inhibitor SP600125 (JNKi), a compound previous reported to

block myelin dismantling in Schwann cells in vitro (Gomez-Sanchez et al., 2015). Accordingly, treatment with JNKi strikingly prevented the degradation of myelin ovoids in uninfected and *M. leprae*-infected cells cultured for 3 days, keeping their myelin values similar to those observed in freshly plated uninfected mSCs at 0 hr (Figure 3a-f). After confirming that, we next measured leprosy pathogen content by quantitative polymerase chain reaction (PCR) analysis of *M. leprae* DNA and RNA in infected mSCs treated or not with JNKi (Figure 3g). Remarkably, we found a notable reduction of about 3.3-fold in *M. leprae* content when we prevented myelin degradation inside mSCs. These results provided, for the first time, evidence that myelin breakdown is a major contributor for *M. leprae* persistence in Schwann cells,

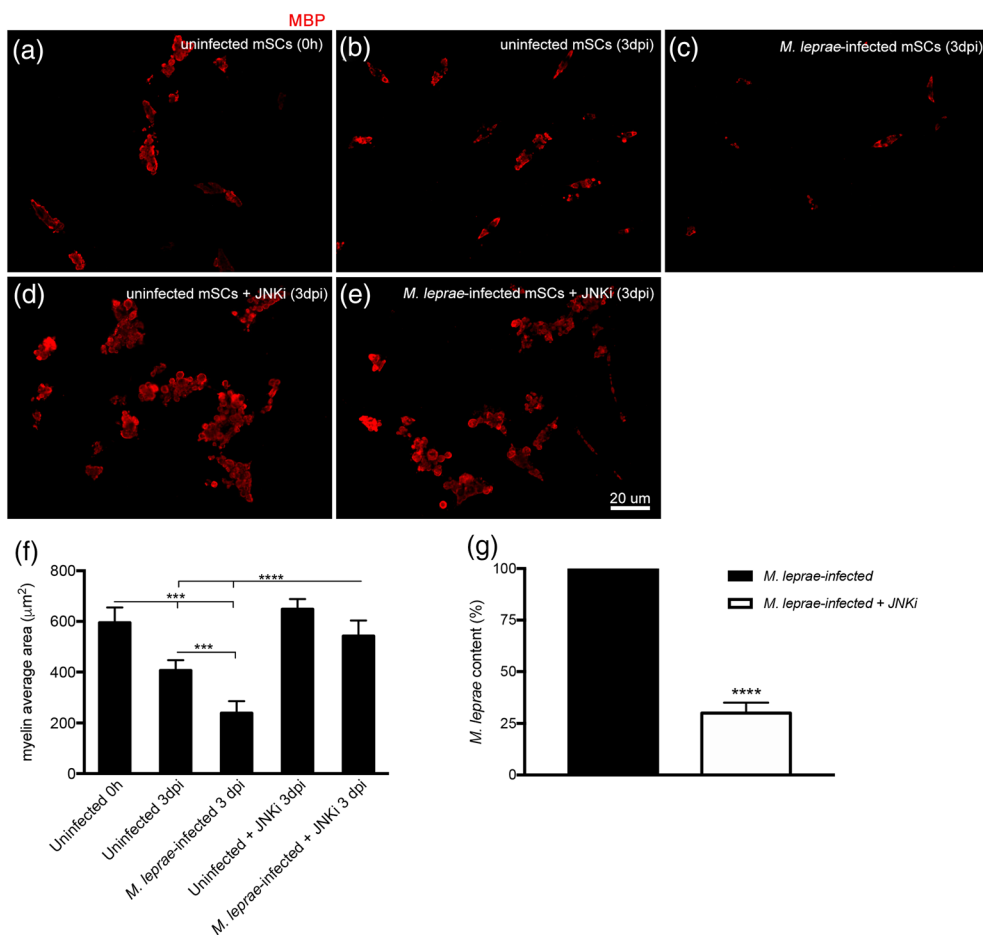


**FIGURE 3** Pharmacological inhibition of myelin breakdown impairs *M. leprae* physiology. (a–e) Immunostaining for MBP in uninfected and *M. leprae*-infected mSCs at different time points and conditions. (f) The graphs show the overall quantification of myelin ovoids in mSCs; results are expressed as mean  $\pm$ SD from three to six independent experiments with at least 200 cells analysed per experiment. (g) The graph shows reduced *M. leprae* content when myelin breakdown was interrupted after JNKi treatment; results are expressed as mean  $\pm$ SD from four independent normalised experiments. \*\* $p$  < .01, \*\*\* $p$  < .001, \*\*\*\* $p$  < .0001

suggesting the pivotal role of myelin dismantling favouring the intracellular survival of leprosy pathogen in the peripheral nerve of infected patients.

### 3 | DISCUSSION

Leprosy neuropathy is considered as the most common peripheral degenerative disorder of infectious origin (Scollard et al., 2015; Serrano-Coll et al., 2018). Increasing number of reports have argued potential mechanisms driven by *M. leprae* in triggering demyelination after contacting myelinated fibres (Madigan et al., 2017; Rambukkana et al., 2002; Scollard et al., 2015; Serrano-Coll et al., 2018; Tapinos et al., 2006). However, the interplay between myelin breakdown and *M. leprae* physiology was entirely ignored. For example, do degenerating myelin byproducts support *M. leprae* viability inside the host cell? In this study, we delineate the hypothesis that myelin breakdown is an advantage strategy induced by *M. leprae* to survive longer intracellularly.

We initially confirmed that *M. leprae* was capable of entering mSCs, a capacity that has not been studied in much detail (Rambukkana et al., 2002). Furthermore, by using our modelling of mSCs-*M. leprae* interaction, we observed a marked affinity of leprosy pathogen for degenerating myelin ovoids. Interestingly, macrophages, after being infected with *M. leprae*, promote nerve demyelination followed by myelin debris phagocytosis (Madigan et al., 2017), which, indeed, provide myelin fragments to the intracellular bacteria. Collectively, we propose a novel unexpected predilection of *M. leprae* for degenerating myelin debris, which are, undoubtedly, major protective lipid-enriched shelters inside the host cell. Future biochemical studies will also help elucidate this metabolic partnership, as it appears plausible that *M. leprae* would be able to metabolise myelin-derived elements.

The consequence of *M. leprae* infection for the degeneration of intracellular myelin was largely underappreciated. We, therefore, addressed this question and surprisingly found that leprosy infection significantly accelerated the rate of myelin breakdown in a time-dependent fashion. Moreover, this enhancement on myelin digestion was followed by a marked suppression of key myelin-promoting genes, such as MBP, MPZ, and Krox-20 transcripts. Our findings were also

validated in human nerve biopsies from leprosy patients and are consistent with previous reports that documented the shutdown of several myelin genes, including the myelin inductor Krox-20, in *M. leprae*-infected Schwann cells (Casalenovo et al., 2019; Masaki et al., 2013).

In order to understand the underlying mechanisms linked to the advanced myelin breakdown observed in infected mSCs, we turned our attention to the autophagic myelin destruction pathway, namely, myelinophagy. Our data clearly show elevated myelinophagy, at an average of about threefold higher in *M. leprae*-infected mSCs as compared with uninfected ones. This was also confirmed *in vitro* and *in vivo* by the marked upregulation of key transcripts involved in early autophagosome formation. This intricate regulatory phenomenon that digests myelin inside Schwann cell is commonly observed during the nerve injury response, such as trauma (Gomez-Sanchez et al., 2015) and inflammatory disorder (Jang et al., 2016). Here, we provided additional evidence about the involvement of this pathway in an infectious disorder of the peripheral nerve.

Because of the critical importance of lipid droplets for *M. leprae* physiology (Barisch & Soldati, 2017; Mattos et al., 2010, 2012), we therefore wanted to check the formation of these organelles in the *in vitro* modelling of mSCs infection. Indeed, we quantified statistically significant increase in the number of these lipid droplets that were also correlated with a significant 1.6-fold reduction in the overall myelin ovoids size in *M. leprae*-infected mSCs, as compared with uninfected ones, which correlates very well with the acceleration of myelin breakdown and augmented appearance of lipid droplets induced by leprosy bacilli. We corroborated this finding by quantitative PCR analysis that confirmed a marked 8.7-fold upregulation in perilipin mRNA along with a statistical downregulation of about two-fold in both HSL and ATGL in *M. leprae*-infected mSCs. Interestingly, skin lesions of leprosy patients and *M. leprae*-infected macrophages have increased perilipin expression at both mRNA and protein levels (Tanigawa et al., 2008). Importantly, perilipin acts as a scaffold protein promoting lipid droplets synthesis and enlargement (Ikura & Caldwell, 2015; Sun et al., 2014) and preventing lipolysis (Straub, Stoeffel, Heid, Zimbelmann, & Schirmacher, 2008). Collectively, this *M. leprae*-induced elevated myelinophagy is very likely to benefit leprosy pathogen in, at least, two ways. First, activation of myelinophagy is an important core mechanism that promotes Schwann cell reprogramming (Gomez-Sanchez et al., 2015). Second, augmented myelin digestion results in accompanied increased levels of lipid droplets as demonstrated here and in previous reports (Brosius-Lutz et al., 2017; Goodrum et al., 1994).

Because myelin breakdown leads to lipids droplets formation, it is conceivable that *M. leprae* would induce myelin dismantling to ensure lipids availability and, hence, their proper intracellular functioning. Thus, we pharmacologically inhibited myelin degradation and, remarkably, observed a significant 3.3-fold reduction in *M. leprae* content. This novel finding suggests a new unpredictable role of myelin breakdown favouring *M. leprae* in Schwann cells.

In conclusion, we propose that myelin breakdown is an evolutionary advantage strategy perpetrated by *M. leprae* to survive longer in the peripheral nerve. Basic research into a better mechanistic

understanding of this unexpected myelin-*M. leprae* coupling could be used for future host-target therapy strategies to treat patients with leprosy neuropathy.

## 4 | EXPERIMENTAL PROCEDURES

### 4.1 | Myelin degrading Schwann cells culture

All animal procedures were approved by the Oswaldo Cruz Foundation Animal Care Committee (License LA-003/2017) and followed the guidelines of the Brazilian Council on Animal Care. We obtained mSCs from mouse sciatic nerves, as described previously, with minor modifications (Gomez-Sanchez et al., 2015). Briefly, adult male wild type BALB/c mice (1 month old) were euthanised with CO<sub>2</sub>, and both sciatic nerves were dissected and placed in L15 medium on ice. The epineurium was carefully removed, and nerve segments were allowed to degenerate *in vitro* for 2 days at 37°C/5% CO<sub>2</sub> in culture medium containing Dulbecco's modified Eagle's medium/F12 supplemented with 10% fetal bovine serum + penicillin-streptomycin (100 U ml<sup>-1</sup>). Then, nerve segments were enzymatically digested for 18 hr in 0.005% collagenase A (Sigma) + 1.2 U ml<sup>-1</sup> dispase (Gibco) in Dulbecco's modified Eagle's medium/F12 medium at 37°C/5% CO<sub>2</sub> followed by mechanical dissociation with 26G gauge syringe. After centrifugation at 300 g for 5 min, the cells were resuspended in culture medium and plated on laminin-coated coverslips (5 µg ml<sup>-1</sup>, ThermoFisher, #23017015) for 5 hr at 37°C/5% CO<sub>2</sub>. Then, plated mSCs were washed 3× in PBS and the culture medium was replaced. When indicated, mSCs cultures were treated with JNK inhibitor SP600125 at final concentration of 40 µM (Enzolifesciences, #SP600125) diluted in culture medium.

### 4.2 | *M. leprae* purification, labelling, and infection *in vitro*

Suspension of viable Thai-53 strain of *M. leprae* obtained from nude mouse-derived footpad was gently provided by Dr. Rosa Laboratory from Lauro de Souza Lima Institute, São Paulo, Brazil, and was purified as described (Medeiros et al., 2016). For experimental infection, mSCs were incubated with *M. leprae* at MOI ≤1:100 cell per bacilli in the cell incubator set up for 33°C/5% CO<sub>2</sub>. After the desired time points, mSCs were washed, fixed, and processed for either immunolabelling or PCR procedures. When indicated, *M. leprae* labelling was performed using the PKH67 Green Fluorescent Cell Linker Kit (Sigma, #MKCF0773) according to the manufacturer's instructions.

### 4.3 | Immunolabelling, oil red O lipid droplets staining, and apotome microscope

For mSCs immunostaining, cells were fixed with 4% paraformaldehyde in 0.1-M PBS for 15 min, washed 3× in PBS, and then permeabilised in blocking solution containing 0.03% Triton X-100 + 5% normal goat serum + 2% bovine serum albumin in PBS for 1 hr. Then, cells were

incubated 30 min (room temperature) with primary antibodies diluted in blocking solution; rat anti-MBP monoclonal (1:300 Millipore, MAB386) and rabbit anti-LC3 polyclonal (1:100 Novus Biological, NB100-2220). Then, cells were washed 3× in PBS and incubated for another 30 min (room temperature) in blocking solution containing DAPI (1:500, Invitrogen, Molecular Probes) and secondary antibodies, goat anti-rat 488 and goat anti-rabbit 594 (both at 1:500, Invitrogen, Molecular Probes). Then, mSCs were washed 2× in PBS and 1× in distilled water, and slides were mounted in Fluoromount medium (Sigma). Oil red O droplets staining and quantification were performed as described by Rolfe, Bosco, Broussard, and Ren (2017), and myelin ovoids size was measured in bright field images at ImageJ.

All images were examined under a Zeiss AxioObserver Z1 inverted microscope (Carl Zeiss, Heidenheim, Germany) with an apotome structured illumination system, using a Zeiss Plan-Apochromat 40×-oil and/or 63×-oil objectives. Excitation was achieved using HXP-120 light source, and images were acquired using a Zeiss HMRC charge-coupled device camera controlled by AxioVision version 4.8 software.

#### 4.4 | Quantitative reverse transcription-PCR and *M. leprae* content

Total RNA was isolated from mSCs cultures and human nerve biopsies using Trizol reagent following the manufacturer's instruction. The cDNA was reverse transcribed with SuperScript III First-Strand Synthesis Kit (Invitrogen, #18080-400) and amplified using the SYBR Green PCR Master Mix (Applied Biosystems, Foster City, CA). For mouse mSCs quantitative reverse transcription-PCR (qRT-PCR) analysis, we used the following specific primers pairs as follows: MBP (forward AATCGGCTCACAGGGATTCA and reverse TCCTCCCCAGCTTAA AGATTTGG); MPZ (forward CGGACAGGGAAATCTATGGTGC and reverse TGGTAGCGCCAGGTAAAAGAG); Krox20 (forward AGGCC CTTGACCAGATGA and reverse AAGATGCCGCACTCACAAT); Beclin-1 (forward GCCTGGGCTGTGGTAAGTAA and reverse CCAGCCT CTGAACTGGACA); Wipi2 (forward GCTGTTGGTAGTAAGTCCGGG and reverse GCTTGAGGCTGACAATGGC); ULK1 (forward TGCGCATA GTGTGCAGGTAG and reverse AACATCGTGGCGCTGTATGA); HSL (forward TCGGGGAGCACTACAAACG and reverse CACGCAACTC TGGGTCTATGG), ATGL (forward GGTGCCAACATTATTGAGGTG and reverse AAACACGAGTCAGGGAGATGC); and perilipin (forward GTCC CTATCCGATGCCCTGAAG and reverse GCGTCCGCCTGCTGAAG). For human nerves qRT-PCR analysis, we used the Human Autophagy PCR Array Kit (Genome, #HATPL-I) and Human Schwann Cell Biology PCR Array Kit (ScienCell Research Laboratories, #GK096). All qRT-PCRs were done in triplicate and performed in a StepOnePlus Real-Time PCR System (Applied Biosystems, MA, USA), and the results were analysed by the  $\Delta\Delta CT$  method after normalisation with the housekeeping gene GADPH (forward TGCACCACCAACTGCTTAG and reverse GGATGCAGGG ATGATGTT).

*M. leprae* content was determined using the protocol previously described (Medeiros et al., 2016). Briefly, *M. leprae*-infected mSCs treated or not with JNKi were submitted to DNA and RNA extraction

using Trizol method following the manufacturer's instruction. Total RNA was reverse transcribed using random primers and GoScript Kit (Promega, #A2801) following the manufacturer's instructions. Levels of 16S rRNA were determined and compared against 16S rDNA by TaqMan real-time PCR assay and read on an ABI Step One Plus Sequence Detection System (Applied Biosystems). *M. leprae* content was arbitrarily assumed 100% for the infected mSCs group for comparison against values obtained in the JNK treated *M. leprae*-infected mSCs condition.

#### 4.5 | Statistical analysis

Graphics were generated using Prism version 6.0 software (GraphPad software). Results are presented as the mean  $\pm$  SD and statistically evaluated by Mann-Whitney U test (for qPCR analysis) or t test (for immunostaining analysis). Differences were considered significant at p-value of <.05.

#### ACKNOWLEDGEMENTS

This work was supported by CNPq, CAPES, Fiocruz, and FAPERJ. We thank Dr. Rosa for gently providing the nude mouse-derived *M. leprae*. The data that support the findings of this study are available on request from the corresponding author.

#### CONFLICT OF INTERESTS

The authors declare no competing financial interests.

#### ORCID

Bruno Siqueira Mietto  <https://orcid.org/0000-0002-4172-2670>

#### REFERENCES

- Barisch, C., & Soldati, T. (2017). Breaking fat! How mycobacteria and other intracellular pathogens manipulate host lipid droplets. *Biochimie*, 141, 54–61. <https://doi.org/10.1016/j.biochi.2017.06.001>
- Brosius-Lutz, A., Chung, W. S., Sloan, S. A., Carson, G. A., Zhou, L., Lovelett, E., ... Barres, B. A. (2017). Schwann cells use TAM receptor-mediated phagocytosis in addition to autophagy to clear myelin in a mouse model of nerve injury. *Proceedings of the National Academy of Sciences*, 114(38), E8072–E8080. <https://doi.org/10.1073/pnas.1710566114>
- Casalenovo, M. B., Rosa, P. S., de Faria Bertoluci, D. F., Barbosa, A. S. A., Nascimento, D. C. D., de Souza, V. N. B., & Nogueira, M. R. S. (2019). Myelination key factor krox-20 is downregulated in Schwann cells and murine sciatic nerves infected by *Mycobacterium leprae*. *International Journal of Experimental Pathology*, 100, 1–11. <https://doi.org/10.1111/iep.12309>
- Chrast, R., Saher, G., Nave, K. A., & Verhaegen, M. H. G. (2011). Lipid metabolism in myelinating glial cells: Lessons from human inherited disorders and mouse models. *Journal of Lipid Research*, 52(3), 419–434. <https://doi.org/10.1194/jlr.R009761>
- Cole, S. T., Eiglmeier, K., Parkhill, J., James, K. D., Thomson, N. R., Wheeler, P. R., ... Barrell, B. G. (2001). Massive gene decay in the leprosy bacillus. *Nature*, 409(6823), 1007–1011. <https://doi.org/10.1038/35059006>
- Elamin, A.A., Stehr, M., & Singh, M. (2012). Lipid droplets and *Mycobacterium leprae* infection. *J Pathog*, 361374. <https://doi.org/10.1155/2012/361374>, 1, 10.

- Gomez-Sanchez, J. A., Carly, L., Iruarrizaga-Lejarreta, M., Palomo-Irigoyen, M., Varela-Rey, M., Griffith, M., ... Jessen, K. R. (2015). Schwann cell autophagy, myelinophagy, initiates myelin clearance from injured nerves. *The Journal of Cell Biology*, 210(1), 153–168. <https://doi.org/10.1083/jcb.201503019>
- Goodrum, J., Earnhardt, T., Goines, N., & Bouldin, T. W. (1994). Fate of myelin lipids during degeneration and regeneration of peripheral nerve: An autoradiographic study. *The Journal of Neuroscience*, 14(1), 357–367. <https://doi.org/10.1523/JNEUROSCI.14-01-00357.1994>
- Ikura, Y., & Caldwell, S. H. (2015). Lipid droplet-associated proteins in alcoholic liver disease: A potential linkage with hepatocellular damage. *International Journal of Clinical and Experimental Pathology*, 8(8), 8699–8708.
- Jang, S.Y., Shin, Y.K., Park, S.Y., Park, J.Y., Lee, H.J., Yoo, Y.H., Kim J.K. Park, H.T. (2016). Autophagic myelin destruction by Schwann cells during Wallerian degeneration and segmental demyelination. *Glia*, May;64(5):730-42. <https://doi.org/10.1002/glia.22957>.
- Kaur, G., & Kaur, J. (2017). Multifaceted role of lipids in *Mycobacterium leprae*. *Future Microbiology*, 12, 315–335. <https://doi.org/10.2217/fmb-2016-0173>
- Madigan, C. A., Cambier, C. J., Kelly-Scumpia, J. M., Scumpia, P. O., Cheng, T. V., Zailaa, J., ... Ramakrishnan, L. (2017). A macrophage response to *Mycobacterium leprae* phenolic glycolipid initiates nerve damage in leprosy. *Cell*, 170(5), 973–985. <https://doi.org/10.1016/j.cell.2017.07.030>
- Masaki, T., Qu, K., Cholewa-Waclaw, J., Burr, K., Raauum, R., & Rambukkana, A. (2013). Reprogramming adult Schwann cells to stem cell-like cells by leprosy bacilli promotes dissemination of infection. *Cell*, 152(1-2), 51–67. <https://doi.org/10.1016/j.cell.2012.12.014>
- Mattos, K. A., Lara, F. A., Oliveira, V. G., Rodrigues, L. S., D'Avila, H., Melo, R. C., ... Pessolani, M. C. (2010). Modulation of lipid droplets by *Mycobacterium leprae* in Schwann cells: A putative mechanism for host lipid acquisition and bacterial survival in phagosomes. *Cellular Microbiology*, 13(2), 259–273. <https://doi.org/10.1111/j.1462-5822.2010.01533.x>
- Mattos, K. A., Oliveira, V. G., D'Avila, H., Rodrigues, L. S., Pinheiro, R. O., Sarno, E. N., ... Bozza, P. T. (2011). TLR6-driven lipid droplets in *Mycobacterium leprae*-infected Schwann cells: Immunoinflammatory platforms associated with bacterial persistence. *Journal of Immunology*, 187(5), 2548–2558. <https://doi.org/10.4049/jimmunol.1101344>
- Mattos, K. A., Sarno, E. N., Pessolani, M. C. V., & Bozza, P. T. (2012). Deciphering the contribution of lipid droplets in leprosy: Multifunctional organelles with roles in *Mycobacterium leprae* pathogenesis. *Memórias do Instituto Oswaldo Cruz*, 107(Suppl 1), 156–166. <https://doi.org/10.1590/S0074-02762012000900023>
- Medeiros, R. C., Girardi, K. D., Cardoso, F. K., Mietto, B. S., Pinto, T. G., Gomez, L. S., ... Lara, F. A. (2016). Subversion of Schwann cell glucose metabolism by *Mycobacterium leprae*. *The Journal of Biological Chemistry*, 291(41), 21375–21387. <https://doi.org/10.1074/jbc.M116.725283>
- Petito, R. B., Amadeu, T. P., Pascarelli, B. M., Jardim, M. R., Vital, R. T., Antunes, S. L., & Sarno, E. N. (2013). Transforming growth factor- $\beta$ 1 may be a key mediator of the fibrogenic properties of neural cells in leprosy. *Journal of Neuropathology and Experimental Neurology*, 72(4), 351–365. <https://doi.org/10.1097/NEN.0b013e31828bfc60>
- Rambukkana, A., Zanazzi, G., Tapinos, N., & Salzer, J. L. (2002). Contact-dependent demyelination by *Mycobacterium leprae* in the absence of immune cells. *Science*, 296(5569), 927–931. <https://doi.org/10.1126/science.1067631>
- Rolfe, A. J., Bosco, D. B., Broussard, E. N., & Ren, Y. (2017). In vitro phagocytosis of myelin debris by bone marrow-derived macrophages. *J Vis Exo*, 30(130). <https://doi.org/10.3791/56322>
- Scollard, D. M., Truman, R. W., & Ebenezer, G. J. (2015). Mechanisms of nerve injury in leprosy. *Clinics in Dermatology*, 33(1), 46–54. <https://doi.org/10.1016/j.jcdermatol.2014.07.008>
- Serrano-Coll, H., Salazar-Peláez, L., Acevedo-Saenz, L., & Cardona-Castro, N. (2018). *Mycobacterium leprae* induced nerve damage: Direct and indirect mechanisms. *Pathog Dis*, 76(6). <https://doi.org/10.1093/femspd/fty06>
- Straub, B. K., Stoeffel, P., Heid, H., Zimbelmann, R., & Schirmacher, P. H. (2008). Differential pattern of lipid droplet-associated proteins and de novo perilipin expression in hepatocyte steatogenesis. *Hepatology*, 47(6), 1936–1946. <https://doi.org/10.1002/hep.22268>
- Sun, Z., Gong, J., Wu, H., Xu, W., Wu, L., Xu, D., ... Li, P. (2014). Perilipin1 promotes unilocular lipid droplet formation through the activation of Fsp27 in adipocytes. *Nature Communications*, 4, 1594. <https://doi.org/10.1038/ncomms2581>
- Tanigawa, K., Suzuki, K., Nakamura, K., Akama, T., Kawashima, A., Wu, H., ... Ishii, N. (2008). Expression of adipose differentiation-related protein (ADRP) and perilipin in macrophages infected with *Mycobacterium leprae*. *FEMS Microbiology Letters*, 289(1), 72–79. <https://doi.org/10.1111/j.1574-6968.2008.01369.x>
- Tapinos, N., Ohnishi, M., & Rambukkana, A. (2006). ErbB2 receptor tyrosine kinase signaling mediates early demyelination induced by leprosy bacilli. *Nature Medicine*, 12(8), 961–966. <https://doi.org/10.1038/nm1433>

**How to cite this article:** Mietto BS, de Souza BJ, Pessolani MCV, Lara FA, Sarno EN. Myelin breakdown favours *Mycobacterium leprae* survival in Schwann cells. *Cellular Microbiology*. 2020;22:e13128. <https://doi.org/10.1111/cmi.13128>